Comparative study of $MSr_2RECu_2O_{7+\delta}$ compounds with M = Al, Nb, Fe, Ru, Ga and Co and RE = Eu, Y

Shiva Kumar[a,b,*], Anjana Dogra[a], M. Husain[b], H. Kishan[a], V.P.S. Awana[a]

[a] National Physical Laboratory, New Delhi 110012, India
[b] Department of Physics, Jamia Millia Islamia University, New Delhi 110025, India

A B S T R A C T

Comparative study on various systems originated from $MSr_2RECu_2O_z$ (M-1212; $0 \leq \delta < 1$) compounds (M = Al, Nb, Fe, Ru, Ga and Co and RE = Eu, Y) has been made. The Rietveld refinement is done for all samples on their respective X-ray diffraction (XRD) patterns, which showed that all compounds are crystallized in single phase. While, Nb-, Fe-, Ru- and Al-1212 possess tetragonal *P*4/*mmm* space group structure, the Ga-1212 and Co-1212 are crystallized in orthorhombic *Ima*2 space group. The change of space group from *P*4/*mmm* to *Ima*2 resulted in doubling of unit cell. The buckling angle [Cu2–O2–Cu2 angle] determined, showed that most of the studied samples are under doped and hence they lack superconductivity. Thermogravimetric analysis (TGA) showed the M-1212 compounds to be more stable than widely studied 90 K superconductor Cu-1212 (RE-123). The magnetization behavior of Ga-, Nb- and Al-1212 follows a Curie–Weiss like behavior due to paramagnetic contribution of Cu. In case of Co-, Fe-1212 short magnetic correlations/spin-glass like features is seen below 100 K. Different surface morphologies have been observed from the scanning electron microscopy (SEM) study of all the samples. Efforts are underway to dope mobile carriers in studied single phase under doped M-1212 (M = Ga, Nb, Fe, Al and Co) compounds and to introduce superconductivity in them.

1. Introduction

The crystal structure of a material largely determines its physical properties. The structures of M-1212 compounds are derived from RE-123 ($REBa_2Cu_3O_7$ RE = rare earths), which have an orthorhombic (*Pmmm*) structure. Complete replacement of Cu-O_x layer in RE-123 structure by other metal oxide (MO_x) layers results in M-1212 structure. The superconductivity can be possibly introduced in these cuprates by carrier doping in CuO_2 planes by controlling the oxygen stoichiometry in MO_x chains/planes or by replacing M with aliovalent elements. Also there is a variation in crystal structure of these M-1212 compounds with different M. Basically the Cu-O_x chains of Cu-1212 (RE-123) are replaced by GaO_4, CoO_4 and AlO_4 tetrahedra in Ga-1212 [1,2], Co-1212 [3] and Al-1212, respectively. In Ru-1212 and Nb-1212, Cu-O_x chains of RE-123 are replaced by RuO_6 and NbO_6 octahedra. Instead of popular *Pmmm* space group for RE-123, the Ga-1212 and Co-1212 crystallize in orthorhombic *Ima*2 space group [1–5,8–10]. There are reports of the presence of complicated superstructures due to the ordering of two types of MO_4 (M = Ga, Co)-tetrahedra chains L-and R-chains where the tetrahedra rotate in different ways [11–13]. This causes the doubling of *a*-parameter and $\sqrt{2}$ time enlargement in *b*- and *c*-parameters [14]. On the other hand Fe-1212, Nb-1212, Ru-1212 and Al-1212 crystallize in tetragonal *P*4/*mmm*.

Superconductivity has been introduced in Ga-1212 [1–2] and Co-1212 [3–4] by Ca/Mg-doping at RE site and annealing in ultra high O_2-pressure. There are some reports [5–8] which deal with structure and physical properties of Fe-1212 with various elements (Y, Gd and Ba) on RE site. In Fe-1212, Fe having variable valency occupies Cu site of both Cu–O chains (Cu1) and of CuO_2 planes (Cu2) [5] resulting non-superconducting Fe-1212 in as synthesize state. It has been made superconducting by first annealing in reducing atmosphere around 800 °C and then in O_2 flow at 350 °C [8,15]. In Ru-1212 both ferromagnetism and superconducting phenomena simultaneously exists at microscopic level. Here RuO_2 planes are responsible for magnetic ordering, whereas the CuO_2 planes for the superconductivity [16–17]. The formation kinetics of Ru-1212 with Gd at RE site has been explored in Ref. [17]. Existence of superconductivity in Fe- and Ru-based cuprates indicates that superconducting properties are much more sensitive to local structural disorder than to magnetic interactions [8,15,16]. The synthesizing conditions are also the key player to realize the

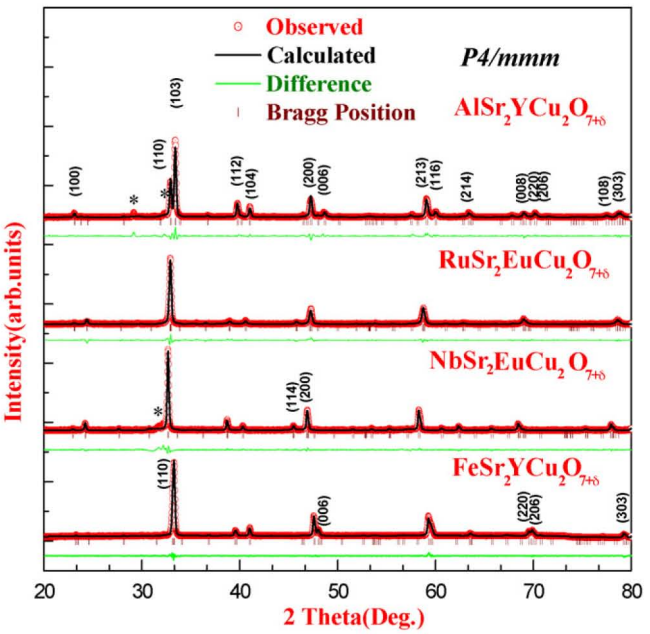

Fig. 1. Rietveld refined XRD pattern of air annealed $MSr_2RECu_2O_{7+\delta}$ samples with space group *P4/mmm*; M = Fe, Nb, Ru and Al; RE = Eu and Y. * refers to impurity phase peak.

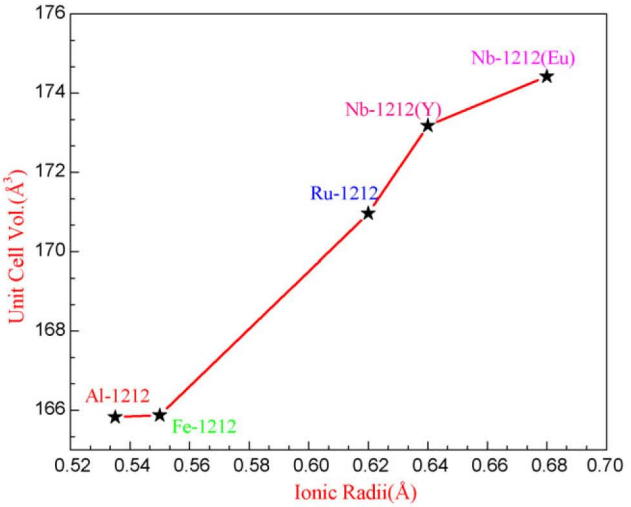

Fig. 2. Variation unit cell volume with ionic radii of M = Al, Fe, Ru and Nb in their respective valence state; RE = Eu and Y.

structure and to make compounds superconducting. The synthesis of Nb/Ru-1212 with heavier rare earths, i.e. $Nb/RuSr_2YCu_2O_8$ requires high-pressure–high-temperature (HPHT) [16], while the $Nb/RuSr_2EuCu_2O_8$ can be with normal solid-state reaction route. In the present article we inter compare the structural details of these systems at one place. The synthesis conditions are optimized for the pure phase compounds and their structural details along with magnetization are reported. The structural details of synthesized M-1212 compounds with M = Nb, Fe, Al, Ru, Ga and Co and RE = Eu, Y demonstrates the versatility of the RE:123 unit cell.

2. Experimental

In the present work we synthesized our samples by solid-state reaction route. All the compositions were prepared by using powders with stated purity better than 99.9%. In case of $GaSr_2YCu_2O_7$, the stoichiometric mixture of Ga_2O_3, $SrCO_3$, Y_2O_3, and CuO was ground thoroughly, calcined at 950 °C for 24 h and then sintered at 980 °C and 1000 °C for 24 h with intermediate grindings. Finally the powder was palletized and re-sintered at 1010 °C for 24 h in air. For $NbSr_2EuCu_2O_8$, the stoichiometric mixture of Nb_2O_5, $SrCO_3$, Eu_2O_3, and CuO was ground thoroughly, calcined at 980 °C for 24 h and then sintered at 1000 °C and 1050 °C in air for 24 h with intermediate grindings. In case of $FeSr_2YCu_2O_8$, the stoichiometric mixture of Fe_3O_4, $SrCO_3$, Y_2O_3, and CuO was ground and calcined at 980 °C for 12 h with subsequent sintering at 1000 °C and 1020 °C in air for 24 h with intermediate grindings. For $AlSr_2YCu_2O_7$, the stoichiometric mixture of Al_2O_3, $SrCO_3$, Y_2O_3, and CuO was ground thoroughly, calcined at 900 °C for 12 h and then sintered at 950 °C and 980 °C for 15 h with intermediate grindings. In composition $RuSr_2EuCu_2O_8$, the stoichiometric mixture of RuO_2, $SrCO_3$, Eu_2O_3, and CuO were ground thoroughly. After first calcination at 1000 °C for 12 h the resultant powder was sintered at 1020 °C. Finally the palletized material was sintered at 1050 °C for 24 h. Similarly for $CoSr_2YCu_2O_7$, the stoichiometric mixture of Co_3O_4, $SrCO_3$, Y_2O_3, and CuO was ground thoroughly, calcined at 900 °C for 12 h and then sintered at 950 °C and 1000 °C for 15 h with intermediate grindings. The final sintering temperature was decided in steps of 20 °C increase every time and the successive X-ray quality of the samples. It is worth mentioning that final sintering temperatures of these compounds vary from 980 °C for Fe-1212 to 1050 °C for Nb-1212. For HPHT synthesis powders of NbO_2, SrO_2, $SrCuO_2$, Y_2O_3 and CuO were taken in stoichiometric ratio. About 300 mg of starting mixture was sealed in a gold capsule and allowed to react in a flat-belt type with the pressure of 6 Gpa at 1200–1300 °C for 3 h, then quenched to room temperature. The HPHT synthesis was done at NIMS Japan. The phase formation was checked for each sample with Rigaku powder diffractometer (Cu-Kα radiation). The X-ray diffraction data were collected at room temperature. The phase purity and lattice parameter, refining was done by Rietveld refinement programme (Fullprof version). The O2–Cu–O2 bond angle were calculated from Rietveld refinement and Gaussian-98 software. The magnetization measurements were carried out on Quantum Design SQUID magnetometer MPMS-XL. The thermogravimetric analysis was carried out on a METTLER TOLEDO TGA/DSC clubbed system.

3. Results and discussion

The M-1212 structure can be viewed as (Ba,Sr)O/CuO_2/RE/CuO_2/(Ba,Sr)O slabs are interconnected through a sheet of M and O with variable composition of MO_x. The oxygen sites in the CuO_2 planes are identified as O2 and O3. The oxygen site in the SrO plane is termed as O4. The MO_x chains/planes oxygen sites are termed as O1 and O5. The RE plane is devoid of oxygen. In tetragonal M-1212 structure oxygen sites O2, O3 and O1, O5 are indistinguishable.

Table 1
Rietveld refined lattice parameters (a, b and c), volume, O2–Cu–O2 angle, occupancy (O1) and Wyckoff positions of $MSr_2RECu_2O_{7+\delta}$ samples with space group *P4/mmm*; M = Nb, Fe, Ru and Al; RE = Eu and Y.

Sample	Nb-1212 (Y)	Nb-1212 (Eu)	Fe-1212	Al-1212	Ru-1212 (Eu)
a (Å)	3.863 (1)	3.873 (2)	3.821 (1)	3.844 (2)	3.845 (2)
b (Å)	3.863 (1)	3.873 (2)	3.821 (1)	3.844 (2)	3.845 (2)
c (Å)	11.605 (7)	11.629 (8)	11.361 (4)	11.221 (3)	11.565 (5)
V (Å^3)	173.177 (3)	174.423 (4)	165.878 (8)	165.831 (4)	170.964 (2)
R_p	4.21	4.12	2.45	4.80	4.18
R_{wp}	5.10	6.30	3.34	7.01	5.55
Chi^2	3.20	4.83	2.20	8.79	4.69
Angle (°) O2–Cu–O2	166.21 (4)	165.18 (4)	165.81 (1)	166.44 (1)	164.30 (5)
Occu. O1	1.916	1.867	1.847	1.893	1.906
Sr(z)	0.196 (3)	0.180 (1)	0.181 (4)	0.193 (2)	0.175 (1)
Cu(z)	0.361 (8)	0.358 (1)	0.350 (4)	0.348 (1)	0.353 (6)
O2(z)	0.389 (1)	0.377 (1)	0.377 (4)	0.364 (8)	0.391 (8)
O3(z)	0.177 (4)	0.156 (5)	0.164 (3)	0.123 (6)	0.180 (1)

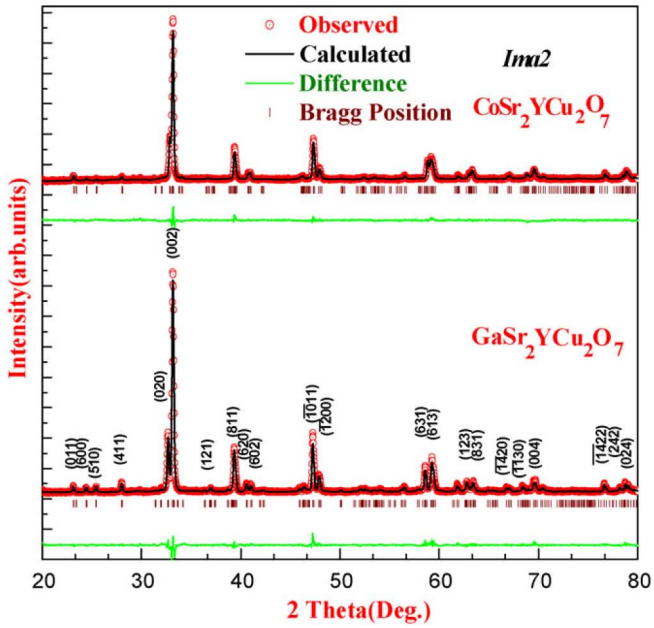

Fig. 3. Rietveld refined XRD pattern of air annealed $MSr_2YCu_2O_{7+\delta}$ samples with space group *Ima*2; M = Ga and Co.

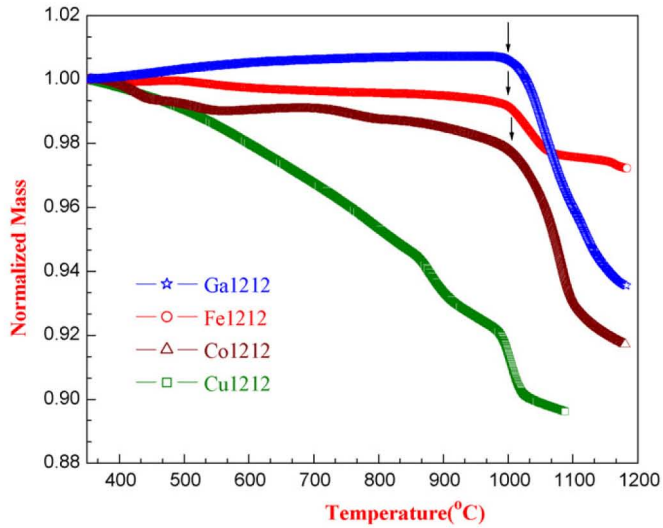

Fig. 4. Variation of normalized mass with temperature in air with heating rate 20 °C per minute. Arrows indicate weight loss occurrence in M-1212 (M = Fe, Ga and Co) after 1000 °C in comparison to Cu-1212.

In case of $MSr_2RECu_2O_{7+\delta}$ (M = Nb, Fe Al and Ru; RE = Y, Eu), all the samples are crystallized in tetragonal *P*4/*mmm* space group. The Rietveld analysis confirmed that the samples to be single phase (Fig. 1). Small impurity peaks are detected in Nb-1212 (Eu) and Al-1212, which may be due to $EuNb_8O_{14}$ (31.71°), $EuNbO_4$ (32.15°) in Nb-1212 (Eu) and $SrAl_2O_4$ (29.16°), $SrAl_4O_7$ (32.30°) in Al-1212. The coordinate positions, lattice parameters and volume for all these samples are tabulated in Table 1 The M atom occupies 1a site with position (0 0 0). Sr with ($\frac{1}{2}$ $\frac{1}{2}$ *z*) have 2 h site and RE (Eu/Y) goes to the site 1d ($\frac{1}{2}$ $\frac{1}{2}$ $\frac{1}{2}$). Cu and O4 occupies 2 g site with position (0 0 *z*). O2, O3 occupies 4i site with position $\frac{1}{2}$ 0 *z* while O1, O5 with site 2f and position (0 $\frac{1}{2}$ 0).

The samples synthesized through HPHT route have smaller lattice parameters and volume than that of the normal pressure solid-state route, see Table 1. This is due to the extreme pressure and lower ionic radii of Y^{3+} (1.019 Å) than Eu^{3+} (1.066 Å) in coordination number (CN = 8). High pressure is necessary for structure formation with Y in case of both Nb and Ru [16]. The refined lattice parameters are in accordance with ionic radii of the M [$Nb^{4+/5+}$ (0.68 Å/0.64 Å CN = 6), Fe^{3+} (0.55 Å low spin, CN = 6) and Al^{3+} (0.535 Å CN = 6)] with their valance and corresponding oxidation states. The lattice parameters are largest for Nb-1212 (Eu) and smallest for Al-1212 [Table 1]. The variation of volume with ionic radii for various studied M-1212 is depicted in Fig. 2. The oxygen content O1 in Nb-1212 (Eu) is slightly less than as in closed cell HPHT synthesized Nb-1212 (Y). For HPHT samples, the oxygen content can be nominally fixed [16]. The Fe-1212 case is more interesting because even though Fe a ferromagnetic element in unit cell still it exhibits superconductivity [15]. But this superconductivity is tricky and happens only when Fe stays at Cu1-chain site [15]. In fact mostly Fe with variable ionic state replaces partly Cu2-plane site up to 47% in oxygen atmosphere and causes disappearance of superconductivity [10]. Slater and Greaves [19] reported that the replacement by Fe at Cu2 site only up to 14%. This shows that the percentage of replacement by Fe at Cu2 site is variable and is dependent on the synthesizing conditions [10,15,19]. However, the well fitted Rietveld refined X-ray diffraction pattern of studied sample shows no replacement by Fe at Cu2 site, see Fig. 1. This could be due to nearly equal scattering factors of Fe and Cu for diffracted X-rays. The neutron diffraction and Mossbauer spectroscopy can only resolve the issue of intermixing of Fe at Cu1 and Cu2 sites

Table 2
Rietveld refined lattice parameters (a, b and c), volume, O2–Cu–O2 angle, occupancy (O1, O5) and Wyckoff positions of $MSr_2YCu_2O_7$ samples with space group *Ima*2; M = Ga and Co.

Sample	Ga-1212	Co-1212
a (Å)	22.797 (1)	22.782 (1)
b (Å)	5.481 (2)	5.451 (1)
c (Å)	5.393 (2)	5.409 (1)
V (Å$^{3)}$	673.861 (1)	671.748 (2)
R_p	3.82	2.32
R_{wp}	4.63	3.12
Chi^2	4.83	2.80
Occupancy (O1, O5)	0.67, 0.35	0.66, 0.34
M(*y*,*z*)	0.25, 0.578 (6), 0.092 (1)	0.25, 0.537 (1), 0.067 (7)
Sr(*x*,*y*,*z*)	0.350 (1), 0.013 (1), 0.047 (1)	0.348 (2), 0.004 (1), 0.004 (2)
Y(*x*,*y*,*z*)	0, 0, 0.041 (1)	0, 0, 0
Cu(*x*,*y*,*z*)	0.427 (4), 0.002 (4), 0.541 (2)	0.426 (8), 0.005 (3), 0.494 (7)
O1(*y*,*z*)	0.25, 0.694 (2), 0.465 (4)	0.25, 0.648 (9), 0.354 (7)
O5(*y*,*z*)	0.25, 0.443 (4), 0.400 (1)	0.25, 0.590 (6), 0.593 (2)
O2(*x*,*y*,*z*)	0.439 (2), 0.789 (5), 0.273 (5)	0.435 (6), 0.742 (2), 0.245 (8)
O3(*x*,*y*,*z*)	0.435 (1), 0.263 (9), 0.753 (1)	0.436 (2), 0.242 (4), 0.747 (9)
O4(*x*,*y*,*z*)	0.330 (8), 0.456 (4), 0.007 (6)	0.324 (1), 0.478 (3), 0.031 (1)

in Fe-1212 structure [10,15,19]. On the other hand aluminium ion replaces Cu1 in Cu-O_x chains with AlO_2 sheets of AlO_4 tetrahedra. The XRD pattern is fitted in P4/mmm tetragonal space group, see Fig. 1. It suggests that AlO_4 tetrahedra are not oriented as GaO_4 and CoO_4 in Ga-1212 and Co-1212 forming L- and R-chains (to be discussed next). HRTEM (high resolution transmission electron microscopy) studies made by Ramirez [12] suggested that these chains are present in Al-1212 as well but in short range ordered form. This also comes out from our Rietveld refinement that position (0.54771) of O1 atom is displaced (Table 1) from mid indicating towards orthorhombic distortion. Seemingly the Al-1212 is border line case between *P*4/*mmm* space group Fe-, Nb-, Ru-1212 and *Ima*2 stabilized Ga-, Co-1212 (to be discussed next).

Unlike the Fe-, Nb-, Ru-1212, the Ga and Co-1212 (Ga-, $CoSr_2YCu_2O_7$) are crystallized in orthorhombic *Ima*2 (No. 46) space group. Rietveld analysis shows good agreement in fitted and observed data, see Fig. 3. The coordinate positions, lattice parameters and volume for these samples are tabulated in Table 2. Y is displaced from (0, 0, 0) site to (0, 0, *z*) site in Ga-1212. Co/Ga, O1 and O5 occupies the $(\frac{1}{4}, y, z)$ position while all the other atoms at the variant (*x*, *y*, *z*) position. The large unit cell can be derived from $6a_p \times \sqrt{2}b_p \times \sqrt{2}c_p$ where a_p, b_p and c_p are the unit cell parameters of normal cubic pervoskite. The unit cell is doubled in comparison to other M-1212 (M = Cu, Nb, Fe, Ru, etc.) structures. This is due to the tendency of the Ga/Co–O planes being arranged in non-centrosymmetrical fashion within one unit cell [3,13]. It can be described as the intergrowth of double rock-salt layers MO_xSrO with double oxygen deficient pervoskite layers of $SrYCu_2O_5$. The lattice parameters (*a* and *b*) of Ga1212, are larger than that of Co-1212, see Table 2. This suggests that Co is in 4+ state because the ionic radii of Ga^{3+} (0.47 Å) is bigger than Co^{4+} (0.40 Å) in existing coordination state of 4. However, there is reverse situation with *c*-parameter, which is due to displacement of Ga from (0, 0, 0) to (0, 0, *z*) position in Ga-1212. Perhaps Ga-1212 indicates distortion towards tetragonal *P*4/*mmm* space group. The results from Tables 1 and 2 clearly indicate towards border line situation for Al-1212 and Ga-1212. Their (Ga-, Al-1212) existing space groups may alter with slight changes in heat treatments. It is clear from our structural refinement results (Figs. 1 and 2 and Tables 1 and 2), that though Fe-, Nb-, Ru-1212 crystallize in *P*4/*mmm* space group, the Co-1212 is clearly crystal-

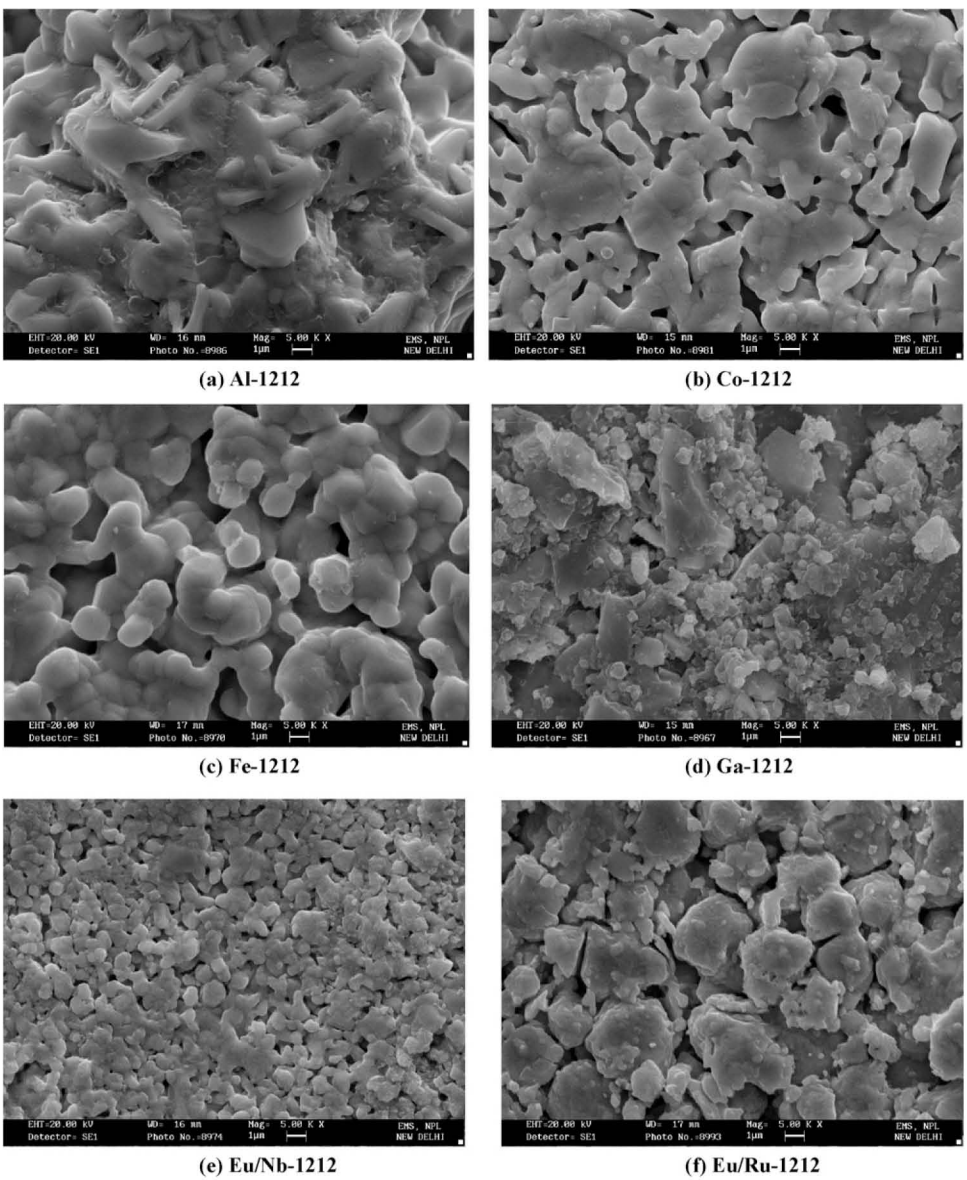

Fig. 5. The scanning electron microscope (SEM) pictures of all the studied M-1212: (a) $AlSr_2YCu_2O_{7+\delta}$, (b) $CoSr_2YCu_2O_7$, (c) $FeSr_2YCu_2O_{7+\delta}$, (d) $GaSr_2YCu_2O_7$, (e) $NbSr_2EuCu_2O_{7+\delta}$, and (f) $RuSr_2EuCu_2O_{7+\delta}$.

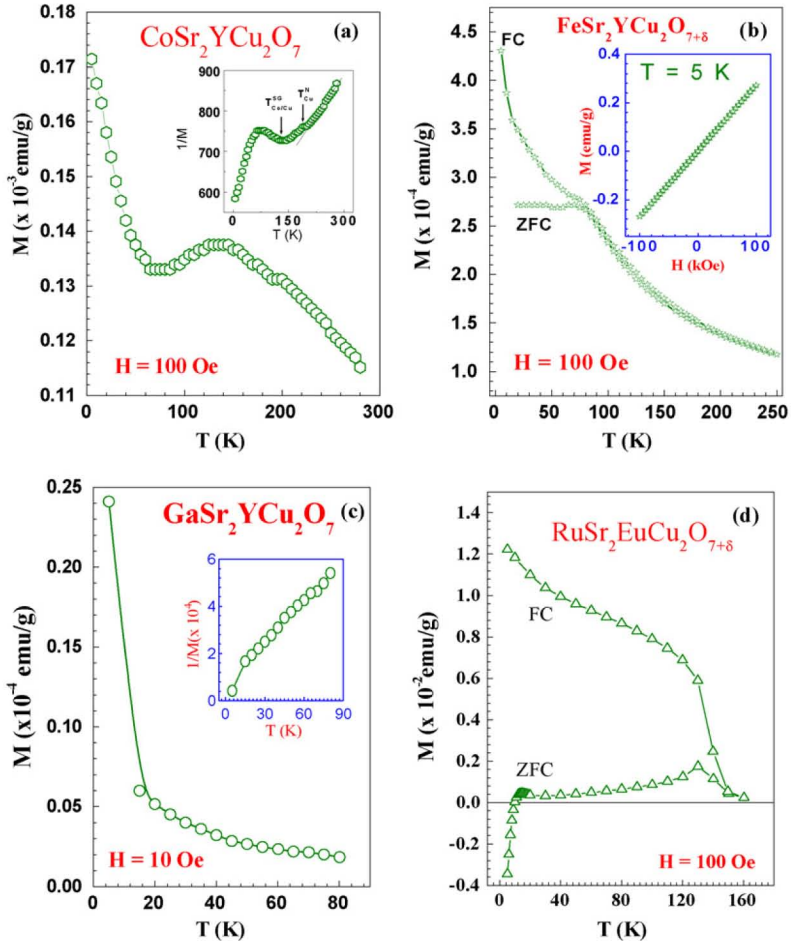

Fig. 6. Magnetization vs. temperature (MT) behavior: (a) $CoSr_2YCu_2O_7$, (b) $FeSr_2YCu_2O_{7+\delta}$, (c) $GaSr_2YCu_2O_7$, and (d) $RuSr_2EuCu_2O_{7+\delta}$. Inset details for (a) $1/M$ vs. T, $CoSr_2YCu_2O_7$, for (b) M-H for $FeSr_2YCu_2O_{7+\delta}$ and for (c) $1/M$ vs. T, $GaSr_2YCu_2O_7$.

lize in *Ima*2 space group. Further the Ga-, Al-1212 are the border line cases with in both space groups, i.e. *P*4/*mmm* and *Ima*2, and could change over from one to another with slight changes in heating schedule, etc.

As number of holes increases in CuO_2 planes, the Cu^{2+} configuration tends to Cu^{3+}. Cu^{2+} configuration in copper-oxide planes results in puckered O2–Cu–O2 bond angles of 165°; Cu^{3+} configuration result in linear bond angle 180° [18]. The O2–Cu–O2 bond angle calculated for various M-1212 samples are given in Tables 1 and 2. All of these are below 170°. This indicates that the samples are under doped and hence can be non-superconducting. But, superconductivity is not related with overall p-type (hole) carriers without putting the right emphasis on structural changes [19–21]. Also, it should be mentioned here the fact that T_c/conductivity increases with holes in CuO_2 planes in oxygen deficient 1212 systems but decreases in fully oxygenated 1212 systems [21–24]. Existence of superconductivity in Ru-1212 is analogous with it see Fig. 6d. We can conclude that samples with M (Ga, Al, Co, Fe and Nb) are under doped and oxygen deficient hence they lack superconductivity. While sample with Ru is although under doped but is oxygenated to that extent that, it can be superconducting. Seemingly the M-O_x blocks in various M-1212 are more robust as stoichiometric M-O_4 (Ga, Al, Co) and M-O_6 (Fe, Nb, Ru) blocks than the versatile carrier reservoir Cu-O_x chains in Cu-1212.

It is known that the Cu-1212 structure being viewed as (Ba,Sr)O/CuO_2/RE/CuO_2/(Ba,Sr)O stacking, possesses variable oxygen in Cu-O_x chains and whereas the other planes such as Ba-O/Sr-O, and Cu-O_2 are oxygen stoichiometric before structural break down. We carried out the thermo gravimetric analysis (weight loss experiments during heating) on various M-1212 samples with M = Cu, Fe, Co and Ga to inter compare the stability of the Cu-O_x chains with that of (Fe, Co, Ga)-$O_{6/4}$ octa/tetrahedrons. The heating is performed in air atmosphere at a rate of 20 °C per minute. The results are shown in Fig. 4. As can be seen from this figure, though the Cu-1212 sample shows substantial weight loss of ~10%, whereas the Fe-, Co- and Ga-1212 are relatively intact and very small weight loss (~2%) is observed till 1000 °C. Even though the three different systems of Fe, Co and Ga show weight loss more or less at same temperature the most stable system out of these three systems seems to be Fe-1212. We can correlate the loss of oxygen with M-O_x blocks/Cu-O_x chains since these blocks/chains are more prone to lose/gain oxygen within their respective unit cell [25,26]. Though these relatively fast runs cannot be used for exact oxygen determinations, the same clearly show the relative stability of M-O_x blocks (weight loss of about 2%) in M-1212 in comparison to the Cu-O_x chains (weight loss of about 10%) in Cu-1212. To know exact oxygen content of these compounds, the slow rate and heavily reduced TGA runs are to be carried out in near future. The same as being done earlier by Matvejeff et al. [26] for Ru-1212 and 1222 compounds. Due to relative better stability of M-O_x blocks in studied M-1212 than the Cu-O_x chains of widely studied 90 K superconductor Cu-1212 (RE-123), the carrier doping is though difficult in the former but if once achieved will be stable than the latter and good for long term practical applications. Our next target is to dope mobile carriers in these stable systems and achieve high temperature bulk superconductivity in them.

The scanning electron microscope (SEM) pictures of all the studied M-1212 samples are depicted in Fig. 5(a–f) at same magnification. In the first Image 5(a) for Al-1212, some sort of melting has taken place. Grains are very much diffused into each other giving rise to a very dense arrangement of the grains. Distinct growth pattern (platelets type) can be observed, which is otherwise not seen in any other images. In case of Co-1212, the grains again look to be well inter-diffused, but the grain formation does not look very distinct. Also the grain size seems to have reduced. This sample looks to be a little more porous than that of the Al-1212. The Fe-1212 shows a very normal grain structure. For this particular sample the growth is in the form of clusters of various grains. There is no systematic grain growth for Ga-1212, in fact few loosely held particles can also be seen in the image. Thus we observe a very broad grain size distribution profile. For the Nb-1212, very uniform narrow grain size distribution is observed. Also the density of the sample is very good and their pore and pore size distribution seems to be very narrow, i.e. uniform. Thus we say that clear grain boundaries can be seen in Co-, Fe-, Nb-1212 [Fig. 5(b), (c), and (e)] and it looks like these bears same morphology except the smaller grain size of Nb-1212 (Eu) system. The Ru-1212 (Eu) sample shows the inhomogeneous grain growth with very poor interdiffusivity, which shows that the sample is porous. More or less it is similar to the Ga-1212 samples. We conclude that since the structure as well as the morphology of all the samples is very much different from each other. Therefore, it might also lead to the variation in other physical properties.

The magnetization behavior of Co-1212, Ga-1212 and Fe-1212 [Fig. 6(a)–(c)] follows a Curie–Weiss like behavior but in different temperature ranges, which are due to paramagnetic contribution of Co, Cu and Fe, spins respectively. In Co-1212 this law is followed in the temperature range of 150–300 K however there is an antiferromagnetic ordering in a very small range near 200 K, which can be due to Cu spins. Below 150 K there is a spin-glass or canted ferromagnetism type broad down-turn is observed in magnetization measurement, which is dominated by the paramagnetic contribution below 50 K [5]. For Fe-1212 the paramagnetic to ferromagnetic transition occurs around 80 K in zero field cooled (ZFC) M-T plot. Interestingly, the field cooled (FC) M-T curve is similar to the results reported by Luo et al. [27] for $x = 0.4$ composition where magnetic properties were correlated with increase in hole concentration of CoO_x layers or increase in charge state of Co. This behavior reveals that most of Fe is in 3+ state which is also much clear from our Rietveld refinement. Similar conclusion has been pointed out in neutron diffraction and Mossbauer study by Karppinen et al. [10] indicating that compound might lack in superconducting charge carriers. There is a weak ferromagnetic ordering in the temperature range 80–60 K but in lower temperature region paramagnetic Fe^{3+} spins take over weak ferromagnetic Fe spins which is also inferred from M-H plot [see inset Fig. 6(b)]. Paramagnetic nature of Ga-1212 compound below 80 K is due to the possible paramagnetic ordering of Cu spins since Ga has non-magnetic nature. The different M-T behavior of Ga-1212 and Co-1212 having same structure indicates that magnetic nature of individual affects whole compound behavior largely in non-superconducting compounds. The magnetization as a function of temperature for Ru-1212 (Eu) at 100 Oe [Fig. 6(d)] shows a clear diamagnetic signal at very low temperature.

4. Conclusions

We synthesized almost single phase samples of 1212 type with different MO_x layers which shows the great flexibility of these rock-salt layers and variable structure formation. With different M, as the oxidation state and ionic state changes, carrier concentration and structure changes as well. While, Nb-, Fe-, Ru- and Al-1212 possess tetragonal *P*4/*mmm* space group structure, the Ga-1212 and Co-1212 are crystallized in orthorhombic *Ima*2 space group. The O2–Cu–O2 bond angle calculation shows samples are under doped and could not be superconducting. The magnetization measurements are also supportive with it in case of some samples. The TGA infers that in the M-1212 compounds M-O_x blocks are much more stable than Cu-O_x chains in Cu-1212. Although the carrier doping is difficult in the former but if once achieved will be stable than the latter and good for long term practical applications. From SEM studies we say that the morphology for all the samples is different from each other.

Acknowledgements

The authors thank to Prof. Vikram Kumar, Director of the National Physical Laboratory, New Delhi, for his constant support and encouragement. One of the authors Shiva Kumar would like to acknowledge CSIR, India for providing fellowships. V.P.S. Awana is also thankful to Prof. E. Takayama Muromauchi for his visit to NIMS, Japan.

References

[1] J.T. Vaughey, J.P. Thiel, E.F. Hasty, D.A. Groenke, C.L. Stern, K.R. Poeppelmeier, B. Dabrowski, D.G. Hinks, A.W. Mitchell, Chem. Mater. 3 (1991) 935.
[2] S. Adachi, S. Takano, H. Yamauchi, J. Alloys Compd. 195 (1993) 19.
[3] Y. Morita, H. Yamauchi, M. Karppinen, Solid State Commun. 127 (2003) 493.
[4] A.A. Khurram, A. Ullah, N.A. Khan, J. Alloys Compd. 481 (2009) 65.
[5] V.P.S. Awana, S.K. Malik, W.B. Yelon, M. Karppinen, H. Yamauchi, Physica C 378 (2002) 155;
V.P.S. Awana, et al., J. Appl. Phys. 93 (2003) 8221.
[6] N. Hassan, N.A. Khan, J. Alloys Compd. 471 (2009) 39.
[7] L.T. Yang, J.K. Liang, G.B. Song, H.F. Yang, H. Chang, G.H. Rao, J. Alloys Compd. 351 (2003) 47.
[8] J. Shimoyama, K. Otzschi, T. Hinouchi, K. Kishio, Physica C 341–348 (2000) 563.
[9] J.M. Tarascon, P. Barbaux, P.F. Mieceli, L.H. Greene, G.W. Hull, M. Eibschutz, S.A. Sunshine, Phys. Rev. B 37 (1988) 7458.
[10] M. Karppinen, V.P.S. Awana, Y. Morita, H. Yamauchi, Physica B 312–313 (2003) 62.
[11] J. Ramirez-Castellanos, Y. Matsui, E. Takayama-Muromachi, M. Isobe, J. Solid State Chem. 123 (1996) 378.
[12] J. Ramirez-Castellanos, Y. Matsui, M. Isobe, E. Takayama-Muromachi, J. Solid State Chem. 133 (1997) 434.
[13] T. Nagai, V.P.S. Awana, E. Takayama-Muromachi, A. Yamazaki, M. Karppinen, H. Yamauchi, S.K. Malik, W.B. Yelon, Y. Matsui, Solid State Chem. 176 (2003) 213.
[14] E. Kandyel, Physica C 415 (2004) 1.
[15] T. Mochiku, Y. Mihara, Y. Hata, S. Kamisawa, M. Furuyama, J. Suzuki, K. Kadowaki, N. Metoki, H. Fujii, K. Hirata, J. Phys. Soc. Jpn. 71 (2002) 790.
[16] V.P.S. Awana, Magneto-superconductivity of Rutheno-cuprates, in: A.V. Narlikar (Ed.), Frontiers in Magnetic Materials, Springer, Berlin, 2005, pp. 531–570.
[17] S. Chen, H.F. Braun, T.P. Papageorgiou, J. Alloys Compd. 351 (2003) 7.
[18] S.R. Ovshynsky, Chem. Phys. Lett. 195 (1992) 455.
[19] P.R. Slater, C. Greaves, Physica C 180 (1991) 299.
[20] O. Chmaissem, J.D. Jorgensen, S. Short, A. Knizhnik, Y. Eckstein, H. Shaked, Nature 397 (1999) 45.
[21] V.P.S. Awana, A.V. Narlikar, Phys. Rev. Lett. 71 (1993) 303.
[22] V.P.S. Awana, A.V. Narlikar, Phys. Rev. B 49 (1994) 6353.
[23] V.P.S. Awana, S.K. Malik, W.B. Yelon, Mod. Phys. Lett. B 10 (1996) 845.
[24] V.P.S. Awana, S.K. Malik, W.B. Yelon, C.A. Cardoso, O.F. de Lima, A. Gupta, A. Sedky, A.V. Narlikar, Physica C 338 (2000) 97.
[25] N.D. Browning, J. Yuan, L.M. Brown, Physica C 202 (1998) 12.
[26] M. Matvejeff, V.P.S. Awana, L.Y. Jang, R.S. Liu, H. Yamauchi, M. Karppinen, Physica C 392 (2003) 87.
[27] X.G. Luo, X.H. Chen, X. Liu, R.T. Wang, Y.M. Xiong, C.H. Wang, G.Y. Wang, Phys. Rev. B 70 (2004) 054520.